Heliyon 10 (2024) e30286

Contents lists available at ScienceDirect

Heliyon

journal homepage: www.cell.com/heliyon

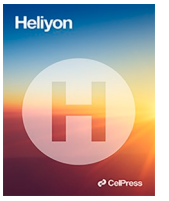

Research article

Effect of tissue fixatives on the corrosion of biomedical magnesium alloys

Guanqi Liu [a,c,1], Ziyu Yan [a,b,1], Yuzhu Guo [a,c], Chuanbin Guo [b], Chengwen Tan [c], Jianhua Zhu [b,**], Jianmin Han [a,*]

[a] *Central laboratory, Peking University School and Hospital of Stomatology, National Center for Stomatology, National Clinical Research Center for Oral Diseases, National Engineering Research Center of Oral Biomaterials and Digital Medical Devices, Beijing Key Laboratory of Digital Stomatology, NHC Key Laboratory of Digital Stomatology, NMPA Key Laboratory for Dental Materials, Beijing, 100081, China*

[b] *Department of Oral and Maxillofacial Surgery, Peking University School and Hospital of Stomatology, National Center for Stomatology, National Clinical Research Center for Oral Diseases & National Engineering Research Center of Oral Biomaterials and Digital Medical Devices, Beijing Key Laboratory of Digital Stomatology, NHC Key Laboratory of Digital Stomatology, NMPA Key Laboratory for Dental Materials, Beijing, 100081, China*

[c] *School of Materials Science and Engineering, Beijing Institute of Technology, Beijing, 100081, China*

ARTICLE INFO

Keywords:
Magnesium alloys
Tissue fixative
Microstructure
Corrosion behavior

ABSTRACT

In this work, the corrosion behavior of pure Mg, Mg3Ag, Mg6Ag, and MgZnYNd alloys in different fixatives (ethyl alcohol (EA), 85 % ethyl alcohol (85 % EA), 10 % neutral buffered formalin (10 % NBF), 4 % glutaric dialdehyde (4 % GD), and 4 % paraformaldehyde (4 % PFA)) was investigated to provide a valuable reference for the selection of fixatives during the histological evaluation of Mg implants. Through the hydrogen evolution test, pH test, and corrosion morphology and product characterization, it was found that corrosion proceeded slowest in the EA and 85 % EA groups, slightly faster in 4 % GD, faster in 10 % NBF, and fastest in 4 % PFA. After corrosion, the EA group surface remained unchanged, while the 85%EA group surface developed minor cracks and warping. The 4%GD fixative formed a dense needle-like protective layer on the Mg substrate. The 10%NBF group initially grew a uniform layer, but later developed irregular pits due to accelerated corrosion. In contrast, the 4%PFA solution caused more severe corrosion attributed to chloride ions. The main corrosion products in the EA and 85%EA groups were MgO and $Mg(OH)_2$, while the other fixatives containing diverse ions also yielded phosphates like $Mg_3(PO_4)_2$ and $MgHPO_4$. In 4 % PFA, AgCl formed on the surface of Mg6Ag alloy after corrosion. Therefore, to minimize Mg alloy corrosion without compromising staining quality, EA or 85 % EA is recommended, while 4 % PFA is not recommended due to its significant impact.

1. Introduction

In the field of biomedical materials, biomedical magnesium (Mg) alloys are frequently used [1,2]. To observe the biological reaction between Mg alloys and the surrounding tissues, precipitate or solidify the substances in the tissues and cells, prevent the cells from autolysis, and maintain cell morphology, Mg alloy implants are usually taken out together with the surrounding tissues and put

* Corresponding authors.
** Corresponding author.
E-mail addresses: zjhsd8811@163.com (J. Zhu), hanjianmin@bjmu.edu.cn (J. Han).
[1] The authors are co-first authors.

https://doi.org/10.1016/j.heliyon.2024.e30286
Received 12 January 2024; Received in revised form 17 April 2024; Accepted 23 April 2024
Available online 25 April 2024

into fixatives, which is convenient for further analysis [3].

To date, various fixatives have been developed to fix different tissues, mainly including aldehydes and ethanol. Aldehydes fix cells by forming cross-linkages within or between proteins [4,5]. Formaldehyde and glutaraldehyde (GD) have their advantages and are the most commonly used aldehyde fixatives. Formaldehyde fixatives, such as neutral formalin (NBF) and paraformaldehyde (PFA), can quickly penetrate tissues and cells, while GD can react rapidly with cell structural proteins, and is mostly used to prepare samples for scanning electron microscopy (SEM) [6]. However, aldehyde fixatives are carcinogenic, and molecular cross-linking can affect the analysis of certain nucleic acids and proteins [7]. Ethanol (EA) fixes and dehydrates tissues, and mostly avoids the damage by aldehydes to macromolecules. However, its penetrating ability is weak, and long-term immersion can easily cause tissue and cells to deform and shrink [8]. Therefore, at present, no one fixative is ideal for all situations, and the fixative should be selected as needed [9].

In addition, a tissue fixative might influence the corrosion of Mg alloys, which may interfere with the evaluation of the quality of sliced staining and implantation efficacy. However, currently, most researchers are mainly concerned about the influence of a corrosive environment *in vivo* or *in vitro* on the corrosion of biomedical Mg alloys [10–12]. When selecting a fixative, researchers usually only consider its influence on tissues, but not on Mg alloy implants, and there have been nearly no such studies on the influence of the storage environment (especially the fixative) on Mg alloy implants. Therefore, it is necessary to explore the influence and mechanism of fixative compositions on Mg alloy corrosion, identify a fixative that meets the requirements of minimal Mg alloy corrosion, and consider the fixing effect on the quality of sliced staining.

In this paper, five commonly used fixatives: EA, 85 % EA, 10 % NBF, 4 % GD, and 4 % PFA, were selected to study the effects of different fixatives and immersion time on the corrosion process of four kinds of Mg alloys (pure Mg, Mg3Ag, Mg6Ag, and MgZnYNd) *in vitro*. This study aimed to provide a theoretical reference for selecting suitable fixatives for biomedical Mg alloys from the corrosion perspective, hoping to obtain more real data from *in vivo* studies.

2. Materials and methods

2.1. Material preparation

For this study, pure Mg (Mg > 99.98 wt%), Mg3Ag (3.0 wt% Ag, Fe < 0.0022 %, Cu < 0.001 %, Ni < 0.001 %), Mg6Ag (6.0 wt% Ag, Fe < 0.0022 %, Cu<0.001 %, Ni < 0.001 %), and MgZnYNd (2.0 wt% Zn, 0.46 wt% Y, 1.0 wt% Nd) were prepared for testing. The materials were all in extruded conditions with an extrusion ratio of 7.1 for pure Mg, Mg3Ag, and Mg6Ag, and 17.4 for MgZnYNd [13,14]. Each kind of material was cut into cylindrical pieces (Φ8 × 2 mm) for study. All the specimens were mechanically ground using silicon carbide (SiC) paper up to 3000 grits and cleaned in ethanol on an ultrasound machine for about 20 min, and then dried in cold air.

2.2. Immersion media

Deionized water was used as the base solution for all immersion media. Pure ethanol (≥99.5 %; Aladdin, Shanghai, China), 36 % formaldehyde in H_2O (Aladdin), 50 % Glutaraldehyde in H_2O (Aladdin), Paraformaldehyde (Aladdin), and inorganic salt were added in deionized water to produce 85 % EA, 10 % NBF, 4 % GD, and 4 % PFA fixatives, respectively. Pure EA was also used as a fixative in this study. The inorganic salt composition of the five fixatives is shown in Table 1. The pH values of 10 % NBF, 4 % GD, and 4 % PFA were adjusted to approximately 7.0.

2.3. Immersion test

The polished and cleaned samples were immersed separately in the five kinds of fixatives at 25 ± 0.5 °C. The volume of the fixative was 20 mL. Three identical samples were tested for each experimental group to ensure the data accuracy.

2.3.1. Hydrogen evolution

During the immersion test, the volume of hydrogen evolved was measured every two days. The sample was covered with a funnel inserted into an inverted burette [12,15]. The H_2 gas produced by the corrosion was collected at the top of the burette by displacing the solution contained in it. The volume of the H_2 evolved was then assessed by noting the level of the fixative inside the burette during the experiment.

Table 1
Inorganic salt composition of five fixatives: EA, 85%EA, 10%NBF, 4%GD, and 4%PFA.

	EA	85 % EA	10 % NBF	4 % GD	4 % PFA
Na_2HPO_4 (g/L)	–	–	6.5	21.18	11.5
NaH_2PO_4 (g/L)	–	–	4	–	2.96
KH_2PO_4 (g/L)	–	–	–	1.4	–
NaCl (g/L)	–	–	–	–	8.5

2.3.2. pH measurements

The pH value of the fixatives was measured using a pH composite electrode (E−201F, Leici, Shanghai, China) every two days, and calibration was carried out in standard buffer solution before each measurement.

2.3.3. Surface and cross-sectional morphology analysis

After 1 and 4 weeks of immersion, the samples without removal of the corrosion products were used directly to assess their morphology by a field-emission scanning electron microscopy (SEM, QUANTA 200F, FEI, Hillsboro, OR, USA/HITACHI SU8220, Tokyo, Japan). After removing the corrosion products, a 3-dimensional (3-D) digital microscope (DVM6A, Leica, Wetzlar, Germany) was used to observe and measure the surface morphology of the sample. A surface roughness curve was drawn on the most corroded area for each corroded sample to indicate the degree of sample corrosion.

2.3.4. Composition analysis

The surface and cross-section compositions of the corrosion product layer were analyzed using an energy-dispersive X-ray spectrometer and a Bruker FlatQuad X-ray spectrometer (Bruker, Billerica, MA, USA). Moreover, X-ray photoelectron spectroscopy (XPS, PHI QUANTERA-II SXM, ULV AC-PHI, Kanagawa, Japan) was used to characterize the composition of chemical elements and chemical states of the sample surface after immersion. The XPS spectra were recorded using Al Kα radiation (1486.6 eV) as the excitation source. The binding energy of the C 1s signal was used to correct the spectra for charging. The background was subtracted using the Shirley method in all spectra. For each immersion parameter, a survey spectrum and high-resolution spectra for C 1s, O 1s, Mg 2p, and P 2p signals were measured. The C 1s narrow scans were fitted using Multi-Pak Software (Gaussian multi-peak fitting; Physical Electronics, Chanhassen, MN, USA).

3. Results

3.1. H_2 evolution of the different fixatives during the immersion test

Fig. 1(a) and (b) show the hydrogen evolution volume and hydrogen evolution rate of four kinds of samples (pure Mg, Mg3Ag, Mg6Ag, and MgZnYNd) in five different fixatives (EA, 85 % EA,10 % NBF, and 4 % GD) over 28 days of corrosion. Fig. 1(c) and (d) are partially enlarged views of the corresponding data.

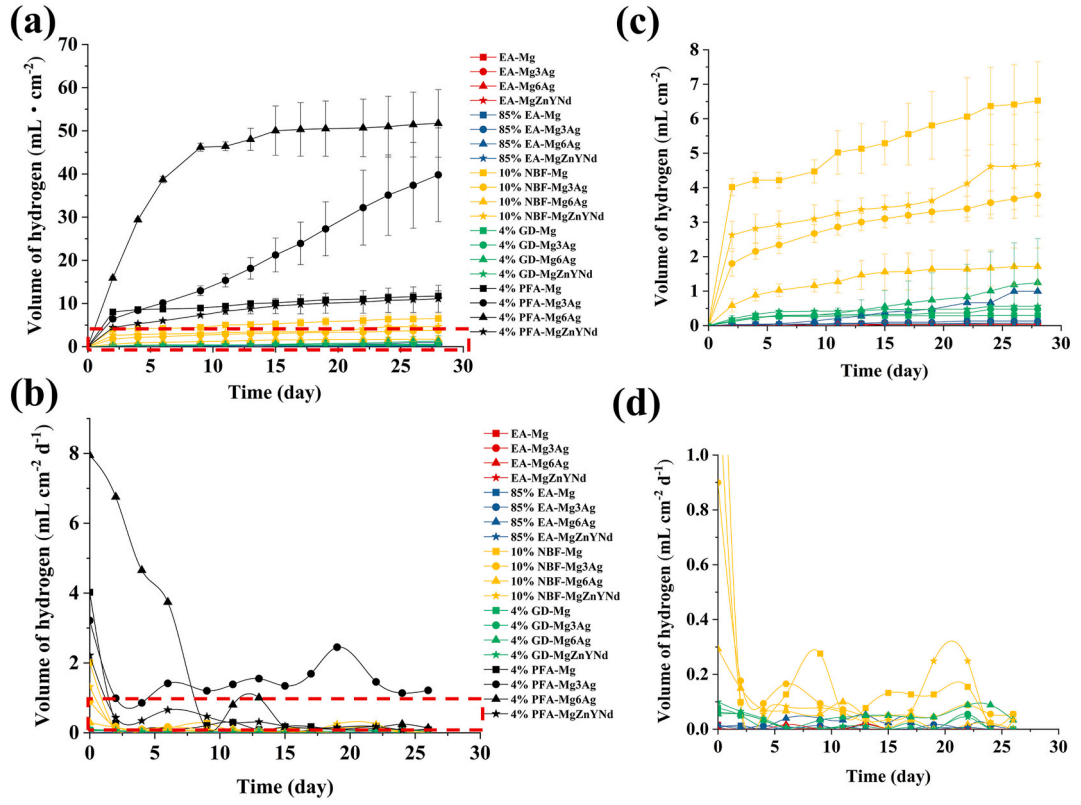

Fig. 1. (a) Hydrogen volume and (b) hydrogen evolution rate released in different fixatives during the immersion test. (c) and (d) are partially enlarged views of (a) and (b), respectively.

In general, during the corrosion process, the hydrogen evolution volume and hydrogen evolution rate of the samples in different fixatives were 4 % PFA >10 % NBF >4 % GD > 85 % EA > EA. The samples immersed in 4 % PFA (2.2–7.9 mL cm^{-2} d^{-1}) and 10 % NBF (0.29–2.0 mL cm^{-2} d^{-1}) had a large hydrogen release rate in the first two days, and the hydrogen release volume also increased rapidly. After two days, the hydrogen release rate decreased rapidly and then fluctuated. The samples immersed in 4 % GD (0.05–0.09 mL cm^{-2} d^{-1}) also had a high hydrogen release rate in the first 6 days, after which the rate decreased rapidly, and then the rate fluctuated. The hydrogen release rate of the sample immersed in 85 % EA was low and the fluctuation range was small during the corrosion period, and the increase in the hydrogen release volume was slow. However, almost no hydrogen evolution was detected in the samples immersed in EA.

Except for the samples immersed in EA, the hydrogen evolution rate of samples immersed in other fixatives was related to the sample composition. For the samples immersed in 4%PFA, 4%GD, and 85%EA, the hydrogen release rate was Mg6Ag > Mg3Ag > Mg ≈ MgZnYNd. Thus, for these three fixatives, the higher the content of Ag, the faster the hydrogen release rate, while other elements like Zn, Y, and Nd might not affect hydrogen release. The hydrogen release rate of Mg6Ag immersed in 4 % PFA decreased after 12 days, which was lower than that of other samples. This is because the Mg6Ag alloy may degrade completely at this time, and there was not enough Mg to react with the fixative. For the samples immersed in 10 % NBF, the corrosion rate was Mg6Ag < Mg3Ag < MgZnYNd < Mg. Moreover, for 10 % NBF, the higher the content of Ag, the slower the hydrogen release rate, while other elements like Zn, Y, and Nd might accelerate hydrogen release.

3.2. pH value of the different fixatives during the immersion test

Fig. 2 shows the changes in the pH value of the 10 % NBF, 4 % GD, and 4 % PFA groups during corrosion, which were added with buffer inorganic salts. The pH values of EA and 85 % EA were not monitored since they cannot be detected by the pH meter. The pH values of 10 % NBF, 4 % GD, and 4%PFA without buffering inorganic salts were 4.5, 3.8, and 9.4, respectively. After adding buffering inorganic salts, the initial pH value of each fixative was close to 7.0.

In the first two days after the immersion test, the pH values of all the 10 % NBF samples increased markedly, and then increased slowly; however, the pH values of the pure Mg and MgZnYNd groups increased significantly after 22 days. The pH value of 4 % PFA immersed with pure Mg and MgZnYNd increased markedly in the first two days and then increased slowly. The change of pH value of 4 % PFA immersed with Mg3Ag could be divided into four stages: the pH value rose rapidly over 0–8 days, increased slowly over 8–14 days, increased again over 14–24 days, and then decreased after 24 days. The pH value of 4 % PFA immersed with Mg6Ag increased sharply (from 6.8 to 10.6) in the first two days, decreased (from 10.6 to 9.87) over 2–8 days, and remained stable after 8 days. The pH values of all 4 %GD samples increased markedly in the first two days, and remained basically unchanged from day 2 to day 22, after which it decreased slightly.

3.3. Surface morphology and composition of the samples after immersion in different fixatives

Fig. 3 shows the surface morphology of the samples after immersion in different fixatives for 1 week and 4 weeks, respectively. After 1 week of immersion, all the samples in the EA group were basically unchanged compared with the non-immersed control group, and clear scratches caused by SiC paper polishing could be seen. In the 85 % EA group, for the pure Mg and MgZnYNd samples, the surface scratches still existed, and some white particles appeared; however, for the Mg3Ag and Mg6Ag samples, the scratches disappeared, and surface cracks and warps appeared. In the 10 % NBF group, the surface of the sample was covered with a cracked corrosion product layer. The crack might have been caused by drying during sample preparation and observation. In the 4 % GD group, the surface of the sample was covered with a regular needle-like layer. In the 4 % PFA group, the surface of the pure Mg sample was covered with a fine cracked corrosion product layer. While in the Mg3Ag sample, a larger degree of cracking of the corrosion product layer was observed. The surface of the Mg6Ag sample was covered with an irregular corrosion product layer, and many holes appeared as a result of local corrosion. The corrosion product layer on the surface of the MgZnYNd sample was very thin, and clear scratches and

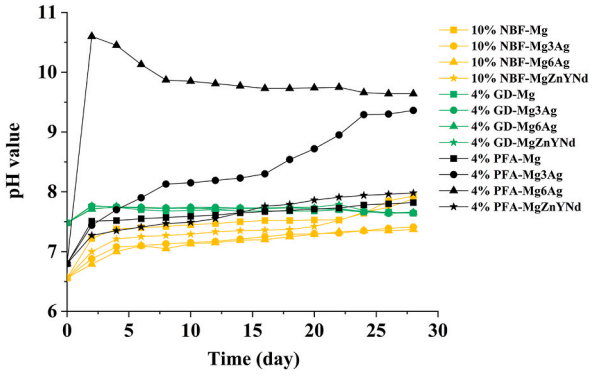

Fig. 2. The pH values of different fixatives during the immersion test.

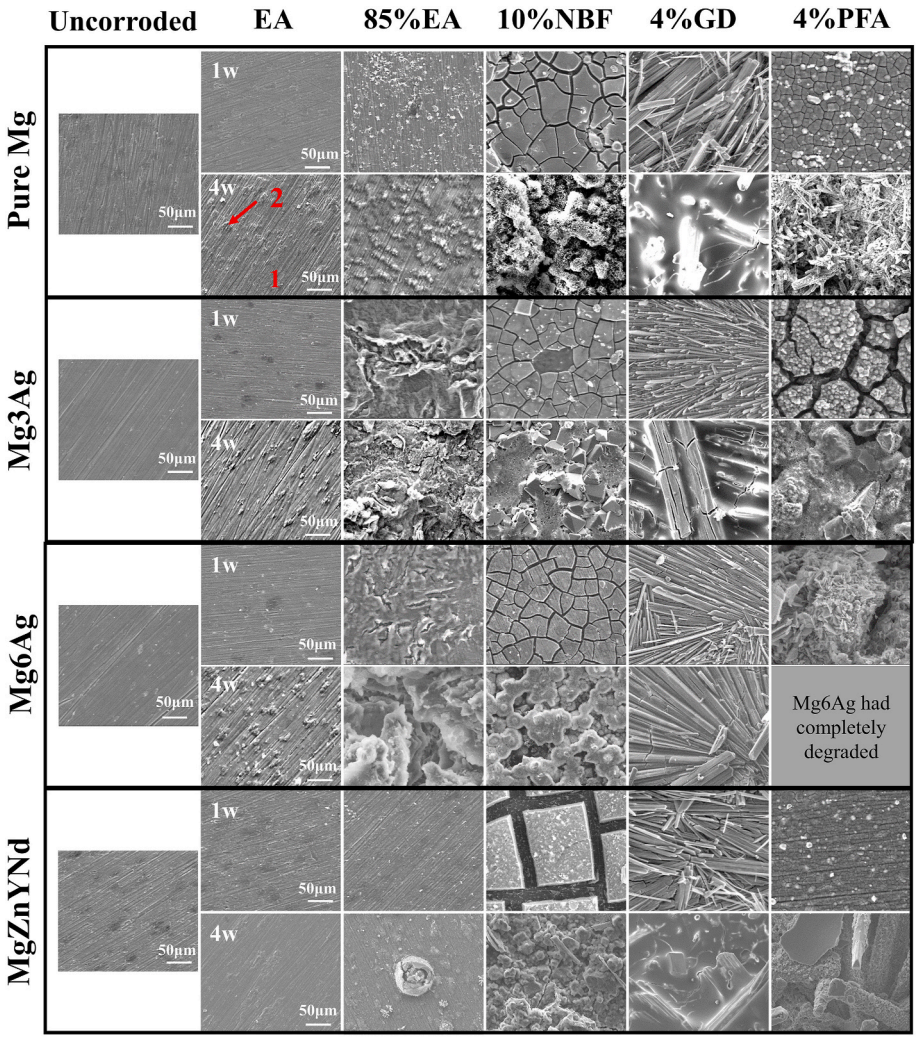

Fig. 3. Scanning electron microscopy images of the sample surfaces after immersion in different fixatives for 1 week and 4 weeks.

cracks could still be seen.

After 4 weeks of immersion, the surface of the samples had changed greatly. In the EA group, the scratches on the surfaces of the pure Mg, Mg3Ag, and Mg6Ag samples were more prominent, and bumps were distributed along the scratch direction. The composition of the bumps and nonbumps was analyzed using energy-dispersive X-ray spectroscopy (EDS), as shown in Table 2. The results showed that the O content in the bumps was higher, and it was preliminarily determined that Mg alloys formed oxides during immersion in EA. For the MgZnYNd samples, only a few bumps distributed on the surface were observed, indicating a lower degree of oxidation. In the 85 % EA group, with the increase of Ag content, the corrosion of the pure Mg, Mg3Ag, and Mg6Ag samples became more serious. The bumps on the surface of pure Mg became dense and there were fine cracks on the bumps. The surfaces of the Mg3Ag and Mg6Ag samples were completely cracked, and the surface of the MgZnYNd sample was partially corroded and cracked. The corrosion product

Table 2
Energy-dispersive X-ray spectroscopy results of the surface position 1 and 2 for pure Mg samples after immersion in ethanol (EA) for 4 weeks.

Position	Element	wt.%	at.%
1	C	5.85	10.12
	O	21.37	27.73
	Mg	72.28	62.15
2	C	1.88	3.04
	O	44.70	54.28
	Mg	53.42	42.68

layer on the surface of the Mg alloys in the 10 % NBF, 4 % GD, and 4 % PFA groups became more irregular than those with 1-week immersion. For 10 % NBF and 4 % PFA groups, more corrosion pits appeared, and it's worth noting that the Mg6Ag sample in the 4 % PFA group had completely degraded.

Furthermore, the surface chemical composition changes of each sample were analyzed in more detail using EDS. For EA and 85%EA groups, O and Mg elements are mainly concerned. As shown in Fig. 4(a), in the EA group, the O content on the surface of all samples after 4 weeks of immersion was higher than that after 1 week of immersion. The O content of pure Mg immersed in EA remained basically unchanged (increased only by 0.89 at. %), followed by Mg3Ag and MgZnYNd, which increased by 12.76 at. % and 16.82 at. % respectively, and the O content of Mg6Ag increased the most, with 30.85 at. %. The O content of Mg, Mg3Ag, and MgZnYNd immersed in 85 % EA for 1 week was similar to that when immersed in EA for 1 week, and the O content of samples in 85 % EA increased significantly after 4 weeks. However, the O content on the surface of the Mg6Ag sample in the 85 % EA group after 1 week was 34.65 at. % higher than that in the EA group, and there was little difference in the surface O content of the Mg6Ag sample in the two fixatives (EA and 85%EA) after 4 weeks of immersion.

For 10%NBF, 4%GD, and 4%PFA groups, Mg and P elements are mainly concerned. As shown in Fig. 4 (b), in the 10%NBF group, compared with immersion for 1 week, only the content of P on the surface of pure Mg increased obviously after 4 weeks, and the content of other samples changed little. In the 4 % GD group, compared with immersion for 1 week, the element content on the surface of all samples showed little change after immersion for 4 weeks. In the 4 % PFA group, the content of Mg on the surfaces of pure Mg, Mg3Ag, and MgZnYNd samples increased markedly, among which that of Mg3Ag increased by 17.75 at. % at most. However, the P content on the surfaces of the three samples decreased markedly, and the maximum decrease of Mg3Ag was 13.87 at.%.

Fig. 5 shows the XPS results for narrow scans of Mg 2p on the sample surfaces after immersion in five fixatives for 4 weeks. It should be noted that Mg6Ag completely corroded after immersion in 4 % PFA for 4 weeks, thus some powdery corrosion products were selected for detection. The Mg 2p spectrum can be assigned to MgO, $Mg(OH)_2$, $Mg_3(PO_4)_2$, and $MgHPO_4$ according to the previous

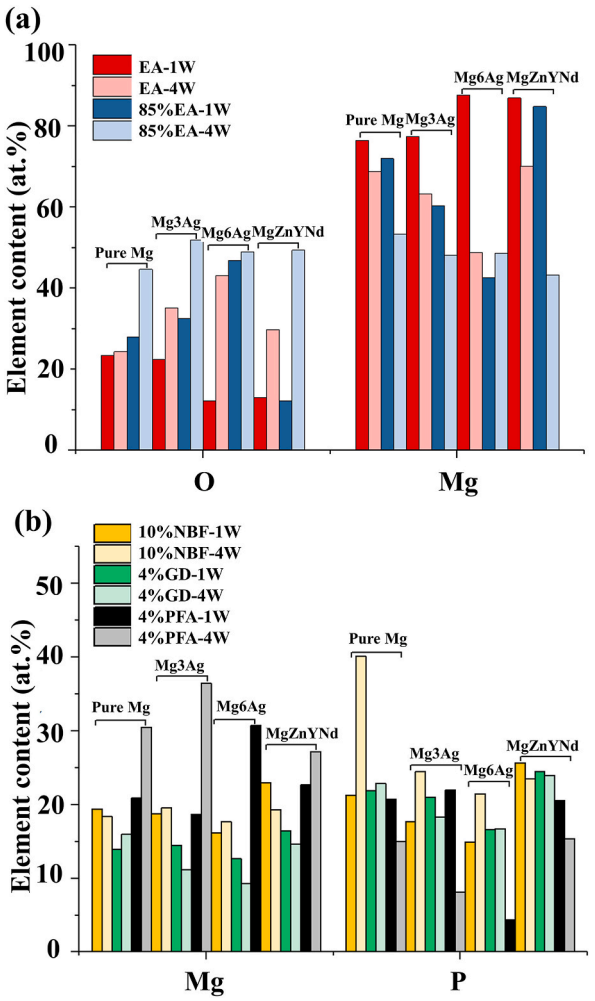

Fig. 4. Energy-dispersive X-ray spectroscopy results of the sample surfaces after immersion in different fixatives for 1 week and 4 weeks: (a) Mg and O element content in EA and 85%EA group, (b) Mg and P element content in 10%NBF, 4%GD, and 4%PFA.

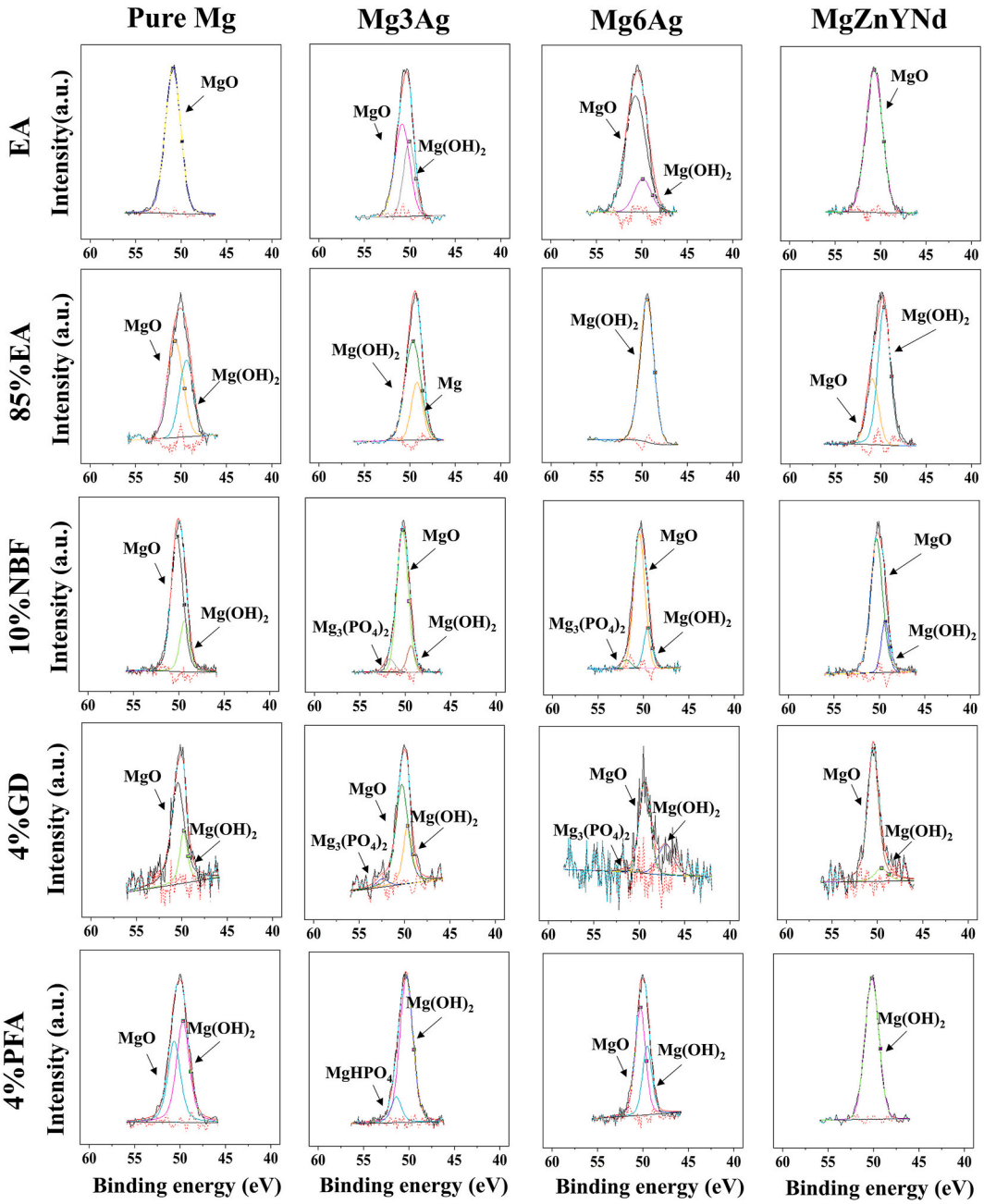

Fig. 5. X-ray photoelectron spectroscopy results using narrow scans of Mg 2p on the sample surfaces after immersion in different fixatives for 4 weeks (Black solid line: measured curve, red solid line: total fitting curve, other solid lines: fitting curves of various substances, and red dotted line: error between fitting value and measured value). (For interpretation of the references to colour in this figure legend, the reader is referred to the Web version of this article.)

researches [16–18]. As shown in the figure, in the EA group, only MgO was detected on the surfaces of the pure Mg and MgZnYNd samples, while MgO and Mg $(OH)_2$ were detected on the surfaces of the Mg3Ag and Mg6Ag samples. This is because alcohol absorbs moisture in the air, and materials with poor corrosion resistance, such as Mg3Ag and Mg6Ag, react with H_2O to generate Mg $(OH)_2$. In the 85 % EA group, Mg $(OH)_2$ was formed on the surface of all samples, which may indicate that Mg alloys were more seriously corroded in 85 % EA.

For the 10 % NBF, 4 % GD, and 4 % PFA groups, except for MgO and Mg $(OH)_2$, $Mg_3(PO_4)_2$ was detected on the surfaces of the Mg3Ag and Mg6Ag samples in the 10 % NBF and 4 % GD groups, and $MgHPO_4$ was detected on the surfaces of Mg3Ag in the 4 % PFA groups. This indicated that Ag-containing Mg alloys were more likely to react with the phosphate. However, only MgO and Mg $(OH)_2$

were detected on the surfaces of the pure Mg and MgZnYNd samples. This may be due to that the phosphate products formed on the surface of the two materials were rare, which can not be detected.

Fig. 6 (a) and (b) show the XPS results for narrow scans of Ag 3d and Cl 2p on the sample surfaces after immersion in five fixatives for 4 weeks. Samples with obvious signal peaks were selected for analysis and display. It was found that the signal of elemental Ag [19] could be detected on the surface of the Mg3Ag and Mg6Ag samples immersed in EA and 85 % EA, and the signal of AgCl [19] could be detected on the surface of the Mg6Ag sample immersed in 4 % PFA.

3.4. Cross-sectional morphology and composition of the samples after immersion in different fixatives

Fig. 7 (a) and (b) show the cross-sectional morphology of the samples after immersion in different fixatives for 1 week. The results of 4 weeks are shown in Supplementary Fig. 1. In each figure, the left side is the resin, and the right side is the sample. The middle portion between the sample and the resin is the corrosion product layer with different thicknesses. In some samples, there were gaps between the corrosion product layer and the matrix material or the resin, which was caused by thermal expansion and cold contraction when the samples were embedded.

For pure Mg and all Mg alloys, immersion in EA resulted in no obvious corrosion interface being observed. After immersion for 4 weeks, a slight oxide layer thickness was observed, which might have been caused by the entry of water and oxygen from the air into EA during immersion. The thickness of the corrosion layer varied with different materials. For pure Mg, Mg3Ag, and MgZnYNd, immersion in EA for 4 weeks resulted in slight corrosion, with corrosion layer thicknesses of ~1 μm, ~5 μm, and ~7 μm, respectively. Mg6Ag exhibited a higher degree of corrosion, with a corrosion layer thickness of ~15 μm.

The immersion of pure Mg and MgZnYNd in 85 % EA for 1 week did not result in any significant changes. However, after 4 weeks of immersion, a small amount of corrosion occurred, with a corrosion layer thickness of ~7 μm. In contrast, Mg3Ag and Mg6Ag experienced higher corrosion, and the thickness of the corrosion layer increased with increasing Ag content and immersion time. The

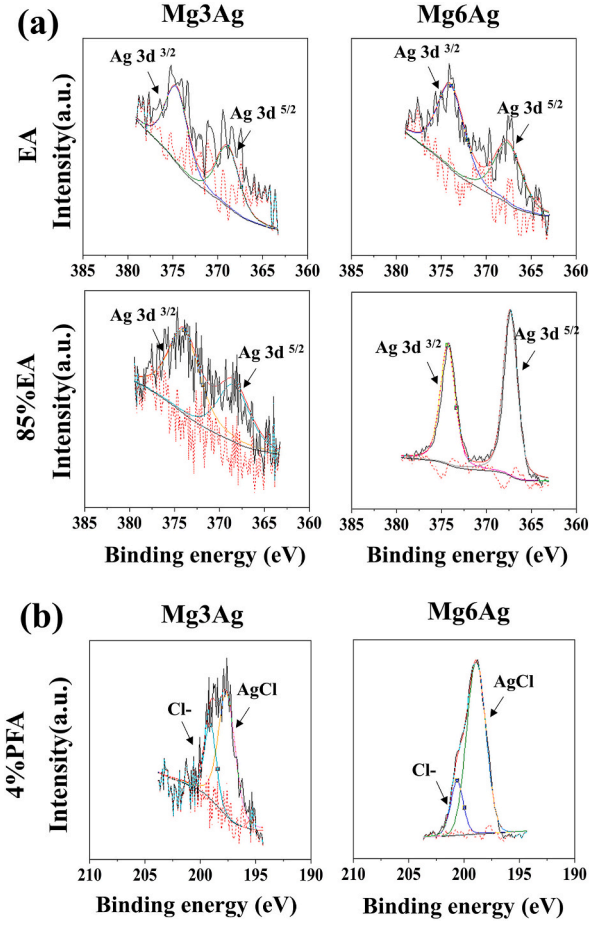

Fig. 6. X-ray photoelectron spectroscopy results using narrow scans of (a) Ag 3d and (b) Cl 2p on the sample surfaces after immersion in different fixatives for 4 weeks (Black solid line: measured curve, red solid line: total fitting curve, other solid lines: fitting curves of various substances, and red dotted line: error between fitting value and measured value). (For interpretation of the references to colour in this figure legend, the reader is referred to the Web version of this article.)

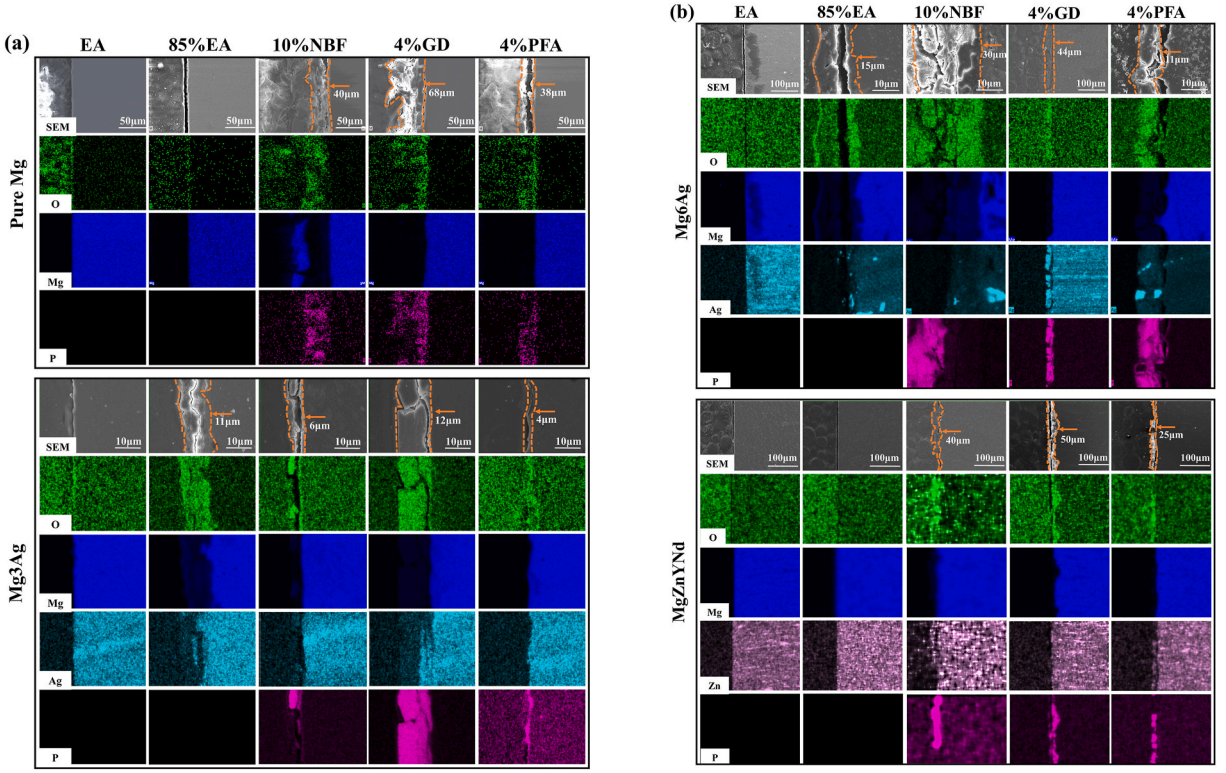

Fig. 7. Energy-dispersive X-ray spectroscopy mapping results of cross-sections of (a) pure Mg, Mg3Ag and (b) Mg6Ag, MgZnYNd samples after immersion in different fixatives for 1 week.

corrosion layer of Mg3Ag increased from ~11 μm after 1 week to ~75 μm after 4 weeks, while that of Mg6Ag increased from ~10 μm to ~140 μm.

When pure Mg and Mg alloys were immersed in 10 % NBF, 4 % GD, and 4 % PFA solutions, the HPO_4^{2-} and $H_2PO_4^-$ in the solutions combined with the Mg^{2+} generated by material degradation to form corrosion products with low solubility, such as $Mg_3(PO_4)_2$, $MgHPO_4{\cdot}H_2O$, and $Mg_3(PO_4)_2{\cdot}H_2O$, which could cover the sample surface [20]. Therefore, a corrosion product layer containing P elements could be observed on the cross-section of the samples. The corrosion layer was thin and loose after 1 week of immersion, and became thickened but remained loose after 4 weeks of immersion in 10 % NBF and 4 % PFA solutions. However, the corrosion layer slightly thickened and became denser in the samples immersed in 4 % GD, which might be one of the reasons for the slower corrosion rate of samples in 4 % GD.

In 10 % NBF, after 1 week of corrosion, the corrosion layer thickness of pure Mg, Mg6Ag, and MgZnYNd alloys ranged between 30 and 40 μm, except for Mg3Ag, which had a corrosion layer thickness of only ~6 μm. After 4 weeks of corrosion, the thickness of the corrosion layer increased for all materials. The layer thickness of pure Mg increased by ~70 μm, while those of Mg3Ag, Mg6Ag, and MgZnYNd increased by ~40 μm. Notably, except for pure Mg, the other three Mg alloys had an elongated and intermittently fractured corrosion layer near the substrate after 4 weeks of immersion. This layer showed an enrichment of alloying elements: Mg3Ag and Mg6Ag had an enrichment of Ag in this layer, while MgZnYNd had an enrichment of Zn. On the top of the alloying element enrichment layer, Mg6Ag also had a dense corrosion layer rich in P deposited on the surface, while Mg3Ag did not have such a corrosion layer, and this P-rich corrosion layer on the surface of MgZnYNd was relatively loose.

In 4 % GD, after 1 week of immersion, a corrosion layer appeared on the surface of the samples, and after 4 weeks, the corrosion layer on all surfaces became denser. Except for MgZnYNd, the corrosion layer on the surfaces of the other three materials increased to varying degrees. The corrosion layer of pure Mg increased from ~68 μm after 1 week to ~120 μm after 4 weeks, while the corrosion layer of Mg3Ag increased from ~12 μm after 1 week to ~90 μm after 4 weeks.

In 4 % PFA, the corrosion rate of all materials was fast, especially for Mg3Ag and Mg6Ag. In the cross-sectional morphology, the corrosion layer on the surface of pure Mg increased from ~38 μm after 1 week of immersion to ~100 μm after 4 weeks of immersion; however, the corrosion layer was loose, and a corrosion crack that extended into the material could be observed in the sample after 4 weeks of immersion. Mg3Ag had a ~4 μm-thick corrosion layer on the surface after 1 week of immersion, while the obvious "corrosion layer" disappeared after 4 weeks of immersion, leaving a corroded sample of ~150 μm thick. From the mapping results, it can be seen that P elements appeared inside the material, indicating that significant corrosion has occurred within the material. Mg6Ag had an ~11 μm porous corrosion layer after 1 week of immersion, and after 4 weeks of immersion, the material had completely degraded, with a large amount of black precipitate in the fixative (XPS analysis showed it to be elemental Ag). The corrosion layer on the surface of

MgZnYNd increased from ~25 μm after 1 week to about ~130 μm after 4 weeks. For the 4-week immersion sample, the corrosion layer could be divided into two parts: a dense Zn-enriched layer on the surface of the material substrate, which was ~60 μm thick, and a corrosion layer rich in P, which was~70 μm thick.

3.5. *Surface morphology of the samples after removal of the corrosion products*

The surface morphology of the samples after removal of the corrosion products was observed using a 3D digital microscope, and the results are shown in Fig. 8. The values in each figure are the maximum height difference on the surface. If the measurement exceeds 50 μm, it is highlighted in red to signify the possible presence of significant corrosion. In the EA group, the morphology of the samples after immersion for 1 week did not change significantly, and the scratches produced by the sandpaper on the surface were visible. After immersion for 4 weeks, the scratches were still visible, and there were some dark, spot-like areas on the surface, which were caused by the absorption of moisture and oxygen in the air by EA, resulting in slight oxidation and corrosion of the Mg alloy. In the 85 % EA group, the situation was similar, and the degree of oxidation and corrosion was more severe than in the EA group, especially for samples after 1 week of immersion, in which the surface scratches were almost invisible. For samples immersed in 10 % NBF, 4 % GD,

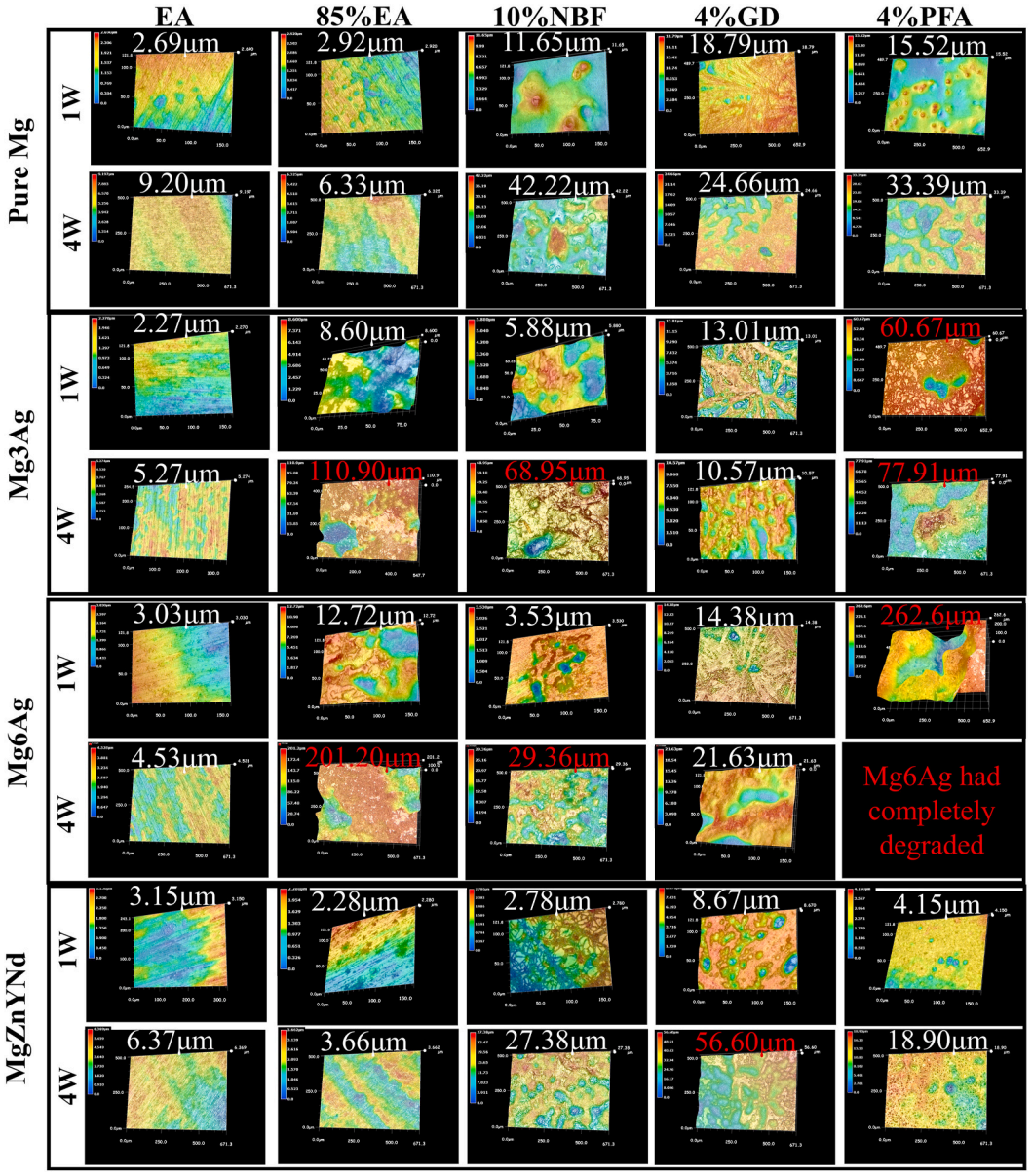

Fig. 8. Surface morphologies of the samples after removal of the corrosion products after immersion in different fixatives for 1 week and 4 weeks.

and 4 % PFA, the corrosion was more obvious, and the scratches disappeared completely. Overall, the surface of pure Mg was less affected by the fixatives, followed by MgZnYNd. Mg3Ag and Mg6Ag were more sensitive to corrosion in the fixatives, and the higher the Ag content, the more severe the corrosion, except for 10 % NBF. In the 10 % NBF group, the degree of corrosion of Mg3Ag and Mg6Ag was exactly the opposite, which may indicate the lower the Ag content, the more severe the corrosion.

Further measurements of the surface roughness are shown in Fig. 9. The selected lines are all drawn in severely corroded areas in each sample. The larger the surface height differences, the more severe the corrosion of the samples. In the EA group, all samples showed a minimal increase in surface height differences after immersion for 1 week and 4 weeks, at ~2.5 μm. In the 85 % EA group, there was an obvious difference in the height difference among the samples: pure Mg and MgZnYNd showed an increase in height difference of 2.5–3 μm after immersion for 4 weeks, while Mg3Ag increased by ~92 μm and Mg6Ag increased by over 170 μm.

In 10 % NBF, after being immersed for 4 weeks, the surface height difference of pure Mg increased by ~20 μm compared with that after 1 week of immersion (~10 μm). The changes in height difference of Mg3Ag and Mg6Ag were similar to those of pure Mg, or even slightly smaller. The change in height difference of MgZnYNd was relatively small, at only ~5 μm.

Meanwhile, in 4 % GD, the surface height difference of pure Mg, Mg3Ag, and Mg6Ag reached ~20 μm after 1 week of immersion, and there was almost no change after 4 weeks of immersion. The surface height difference of MgZnYNd was ~8 μm after 1 week of immersion, and ~18 μm after 4 weeks of immersion.

In 4 % PFA, the surface height difference of pure Mg was only ~2 μm after 1 week of immersion and reached ~22 μm after 4 weeks of immersion. With the increase in Ag content, the change in surface height difference became larger. Mg6Ag corroded so severely after 4 weeks of immersion that it completely degraded, thus no data could be measured. However, the change in surface height difference of MgZnYNd was very small, increasing only from ~2 μm after 1 week of immersion to ~10 μm after 4 weeks of immersion.

4. Discussion

Mg alloys, as biomedical implant materials, have attracted continuous research attention. Systematic animal experiments are often needed to evaluate the efficacy of implant materials before clinical trials. Tissue section staining, especially hard tissue section staining, can effectively reflect the reaction between implant materials and surrounding tissues, and comprehensively evaluate the biological characteristics of the implant materials. During the section preparation process, the tissues need to be fixed using a fixative; however, pure Mg and Mg alloys will degrade as stored in the fixative, which will lead to deviations between the results of section staining and actual *in vivo* situations [3]. Therefore, it is necessary to study the influence of fixatives on the corrosion of Mg alloys, which can guide the selection of fixatives in animal experiments using Mg alloys to obtain experimental data that resembles the actual implantation situations more closely and accurately.

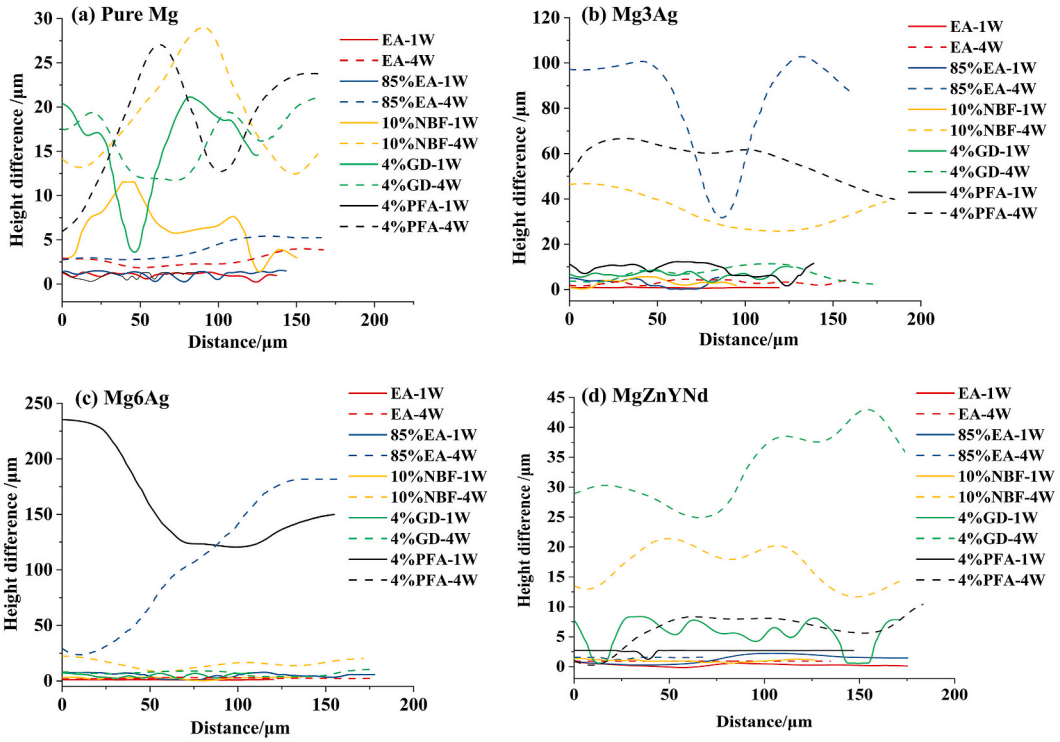

Fig. 9. Surface height differences of (a)Pure Mg, (b) Mg3Ag, (c) Mg6Ag, and (d) MgZnYNd samples after removing the corrosion products after immersion in different fixatives for 1 week and 4 weeks.

This study systematically investigated the influence of five different fixatives on the corrosion behaviors of pure Mg and Mg alloys through pH tests, hydrogen evolution tests, and corrosion morphology and product characterization.

4.1. Corrosion rate

By comparing the corrosion of the same material in different fixatives (as shown in Figs. 1 and 2), it was observed that the material had basically no corrosion in EA, whereas, the material corroded relatively slowly in 85 % EA, while in the other three fixatives (10 % NBF, 4 % GD, 4 % PFA) the materials corroded relatively quickly because of the presence of H_2O. However, among these three fixatives, the material corroded more slowly in the 4 % GD group, probably because the concentration of dihydrogen phosphate ions in the glutaraldehyde fixative is far higher than that in the other fixatives, which could inhibit the severe corrosion of pure Mg and Mg alloys [21,22]. Meanwhile, in the 4 % PFA group, all materials corroded very quickly, which is because sodium chloride is added to polymeric glutaraldehyde, and chloride ions destroy the product layer, thereby accelerating corrosion [23,24].

By comparing the corrosion of the four materials (pure Mg, Mg3Ag, Mg6Ag, and MgZnYNd) in the same fixative (as shown in Figs. 1 and 2), it was found that except for the formaldehyde group, the corrosion of Mg–Ag alloys was faster than pure Mg and MgZnYNd alloy, and the higher the Ag content, the more severe the corrosion. This is caused by the phenomenon of self-catalytic cathodic activation in Mg–Ag alloys. This was first reported by Yang et al. [25], who found that the porous silver-rich dealloying residues and Ag nanoparticles produced in the reaction of Mg–Ag alloys can significantly promote hydrogen reduction, thereby leading to cathodic activation of the material.

In contrast, in the 10 % NBF group, the higher the Ag content, the slower the corrosion of the sample, which occurred because formaldehyde contains free aldehyde groups. In the initial stage of corrosion, Mg first dissolves into Mg^{2+}, the aldehyde groups can reduce the dissolved Ag^{+} in the fixative to elemental Ag [26], allowing elemental Ag to be deposited on the corrosion products, such as magnesium phosphate and magnesium dihydrogen phosphate, making the corrosion product layer denser and further inhibiting corrosion. It was also observed that the outermost layer of Mg6Ag in the formaldehyde group contained a dense P-rich layer, which could also hinder corrosion. Although 4 % GD also contains aldehyde groups, the C–C bonds therein can significantly weaken the reducing ability of the aldehyde groups, thereby diminishing its inhibitory effect on corrosion [27]. 4 % PFA does not have an inhibitory effect on corrosion because PFA does not contain free aldehyde groups [28,29].

4.2. Corrosion morphology and products

By observing the material surface after the immersion experiments, it was found that the surface morphology of the EA group materials remained basically unchanged. In the later immersion period (4 weeks), because of the absorption of a small amount of water from the air by ethanol, the material underwent slight corrosion, which clarified the scratches caused by sandpaper on the surface, along with the generation of a small amount of oxides and hydroxides. The surface morphology of the material in the 85 % EA group changed significantly because of corrosion, with the formation of cracks and curls, which is because 85 % EA contained more water, and pure Mg and the Mg alloys have a more intense corrosive reaction with H_2O, thus leading to the formation of more MgO and $Mg(OH)_2$ on their surfaces.

In addition to formaldehyde, glutaraldehyde, polymeric glutaraldehyde, and other organic components, 10 % NBF, 4 % GD, 4 % PFA also contained inorganic ions (such as H^+, HPO_4^{3-}, $H_2PO_4^{2-}$, Cl^-, etc.) and a higher content of H_2O, all of which significantly affect the corrosion process and cause more severe corrosion of the materials, with large changes in surface morphology. After corrosion, the surface of the 4 % GD group materials formed needle-like corrosion products, which is a typical morphology of phosphates [30,31], and this phosphate product layer was relatively dense and could effectively protect the substrate and hinder corrosion [21,22]. The surfaces of the materials in the 10 % NBF group first formed a uniform corrosion layer, and the observed crack was possibly caused by drying during sample observation. Subsequently, as corrosion progressed, irregularly shaped holes were observed on the material surface, and products such as $Mg_3(PO_4)_2$ were also formed on the surface of the Mg–Ag alloys. The surface of the 4 % PFA group materials also formed a relatively uniform corrosion layer; however, because of the presence of Cl^- in the solution, the corrosion products of the material were relatively loose and porous, and the surface morphology changed dramatically in the later period of corrosion [23,24]. The Mg6Ag alloy almost completely corroded. In addition to Mg phosphates, its surface might also contain corrosion products such as AgCl.

5. Conclusion

This study systematically investigated the corrosion of pure Mg and three Mg alloys in five fixatives, providing an effective reference for selecting fixatives of Mg-based alloy implants. The conclusions are as follows.

(1) For the same pure Mg and Mg alloys, corrosion was slowest in EA and 85 % EA, slightly faster in 4 % GD, faster in 10 % NBF, and fastest in 4 % PFA. Therefore, the EA or 85 % EA with less influence on Mg alloy corrosion is recommended over 4 % PFA with greater influence.
(2) The EA group surface showed little corrosion-induced change and the 85%EA group developed cracks and warping. Hence, the 4%GD fixative formed a dense needle-like protective layer on the Mg substrate. The 10%NBF group initially grew a uniform layer but later irregular pits as corrosion accelerated, and the 4%PFA solution caused more severe corrosion attributed to chloride ions.

(3) The main corrosion products of the materials in the EA and 85 % EA groups were MgO and $Mg(OH)_2$. For the 4 % GD, 10 % NBF, and 4 % PFA solutions which contained a richer variety of ions, phosphates such as $Mg_3(PO_4)_2$ and $MgHPO_4$ were also detected on the surfaces. Additionally, in the 4 % PFA group, AgCl was generated after corrosion of the Mg6Ag alloy which has a higher silver content.
(4) The fixatives were quite sensitive to the Ag content in the Mg alloys, especially in 10 % NBF. The aldehyde groups in the solution could promote the deposition of Ag, forming a protective corrosion layer, thereby hindering the corrosion of the Mg substrate to a certain extent.

Data availability statement

No data was used for the research described in the article.

CRediT authorship contribution statement

Guanqi Liu: Writing – review & editing, Writing – original draft, Methodology, Data curation. **Ziyu Yan:** Writing – original draft, Methodology, Investigation, Formal analysis. **Yuzhu Guo:** Writing – original draft, Methodology, Formal analysis. **Chuanbin Guo:** Supervision, Conceptualization. **Chengwen Tan:** Supervision, Conceptualization. **Jianhua Zhu:** Validation, Project administration, Investigation. **Jianmin Han:** Supervision, Resources, Methodology, Conceptualization.

Declaration of competing interest

The authors declare that they have no known competing financial interests or personal relationships that could have appeared to influence the work reported in this paper.

Acknowledgments

This work was financially supported by the National Natural Science Foundation of China (No. 52171234), the National Key Research and Development Project (Nos. 2019YFE0101100and 2021YFC2400703), National Key Clinical Special Scientific and Technological Achievements Transformation Support Project (No. PKUSSNKP-T202104), Beijing science and technology special key project (No. Z211100002921066), Youth Research Fund, School of Stomatology, Peking University Stomatology Hospital (No. PKUSS20220102) and Postdoctoral Fellowship Program of CPSF (No. GZC20230139).

Appendix A. Supplementary data

Supplementary data to this article can be found online at https://doi.org/10.1016/j.heliyon.2024.e30286.

References

[1] Mostafa M. El-Sayed, A.Y. Shash, Ehab A. El-Danaf, et al., Fabrication of biocompatible Mg-based nano composites by using friction stir alloying, Ceram. Int. 49 (2023) 23476–23490.
[2] Mostafa M. El-Sayed, A.Y. Shash, Ehab A. El-Danaf, et al., Impact of multi-pass friction stir alloying on the characterization of Mg based bio-ceramic nano composites, J. Alloy Compd. 959 (2023) 170477.
[3] B. Ullmann, N. Angrisani, J. Reifenrath, et al., The effects of handling and storage on magnesium based implants-First results, Mater. Sci. Eng. C 33 (2013) 3010–3017.
[4] C.H. Fox, F.B. Johnson, J. Whiting, et al., Formaldehyde fixation, J Histochem, Cytochem. 33 (1985) 845–853.
[5] D. Hopwood, Theoretical and practical aspects of glutaraldehyde fixation, Histochem. J. 4 (1972) 267–303.
[6] F. Zeng, W. Yang, J. Huang, et al., Determination of the lowest concentrations of aldehyde fixatives for completely fixing various cellular structures by real-time imaging and quantification, Histochem, Cell Biol. 139 (2013) 735–749.
[7] J.J. Lou, L. Mirsadraei, D.E. Sanchez, et al., A review of room temperature storage of biospecimen tissue and nucleic acids for anatomic pathology laboratories and biorepositories, Clin. Biochem. 47 (2014) 267–273.
[8] I. Eltoum, J. Fredenburgh, R.B. Myers, et al., Introduction to the theory and practice of fixation of tissues, J. Histotechnol. 24 (2001) 173–190.
[9] D. Hopwood, Fixatives and fixation: a review, Histochem. J. 1 (1969) 323–360.
[10] Y. Li, F. Lu, H.L. Li, et al., Corrosion mechanism of micro-arc oxidation treated biocompatible AZ31 magnesium alloy in simulated body fluid, Prog. Nat. Sci.: Mater. Int. 25 (2014) 516–522.
[11] D.H. Cho, T. Avey, K.H. Nam, et al., In vitro and in vivo assessment of squeeze-cast Mg-Zn-Ca-Mn alloys for biomedical applications, Acta Biomater. 150 (2022) 442–455.
[12] M. Esmaily, J.E. Svensson, S. Fajardo, et al., Fundamentals and advances in magnesium alloy corrosion, Prog. Mater. Sci. 89 (2017) 92–193.
[13] G. Liu, J. Han, X. Yu, et al., Influences of extrusion and silver content on the degradation of Mg-Ag alloys in vitro and in vivo, Bioinorg. Chem. Appl. 2022 (2022) 2557518.
[14] B. Wang, S. Guan, J. Wang, et al., Effects of Nd on microstructures and properties of extruded Mg-2Zn-0.46Y-xNd alloys for stent application, Mater. Sci. Eng. B 176 (2011) 1673–1678.
[15] G. Song, A. Atrens, D. Stjohn, An hydrogen evolution method for the estimation of the corrosion rate of magnesium alloys, in: J.N. Hryn (Ed.), Essential Readings in Magnesium Technology, John Wiley & Sons Inc., Hoboken, 2001, pp. 565–572.
[16] D. Tie, F. Feyerabend, W. Müller, et al., Antibacterial biodegradable Mg-Ag alloys, Eur. Cells Mater. 25 (2013) 284–298.

[17] D.B. Pokharel, L. Wu, J. Dong, et al., Effect of D-fructose on the in-vitro corrosion behavior of AZ31 magnesium alloy in simulated body fluid, J. Mater. Sci. Technol. 66 (2021) 202–212.
[18] M. Liu, S. Zanna, H. Ardelean, et al., A first quantitative XPS study of the surface films formed, by exposure to water, on Mg and on the Mg-Al intermetallics: Al_3Mg_2 and $Mg_{17}Al_{12}$, Corros. Sci. 51 (2009) 1115–1127.
[19] C.D. Wagner, W.M. Riggs, L.E. Davis, et al., Handbook of X-Ray Photoelectron Spectroscopy, Perkin-Elmer Corporation, Waltham, 1979.
[20] S. Rahman, C.M. Navarathna, N.K. Das, et al., High capacity aqueous phosphate reclamation using Fe/Mg-layered double hydroxide (LDH) dispersed on biochar, J. Colloid Interf. Sci. 597 (2021) 182–195.
[21] L. Yang, Y. Shi, L. Shen, et al., Effect of Ag on cathodic activation and corrosion behaviour of Mg-Mn-Ag alloys, Corros. Sci. 185 (2021) 109408.
[22] N. Drogat, R. Granet, V. Sol, et al., Antimicrobial silver nanoparticles generated on cellulose nanocrystals, J Nanopart. Res. 13 (2011) 1557–1562.
[23] L.F. Tietze, T. Eicher, U. Diederichsen, et al., Reactions and syntheses in the organic chemistry laboratory, in: Translated from the German by D. Ringe, University Science Books, Mill Valley, 1989.
[24] S. Patra, A. Kumar, S. Singh, Hydrogen production from formaldehyde and paraformaldehyde in water under additive-free conditions: catalytic reactions and mechanistic, Innorg. Chem. 61 (2022) 4618–4626.
[25] J.A. Kiernan, Formaldehyde, formalin, paraformaldehyde and glutaraldehyde: what they are and what they do, Microscopy Today 8 (2000) 8–13.
[26] L. Hou, N. Dang, H. Yang, et al., A combined inhibiting effect of sodium alginate and sodium phosphate on the corrosion of magnesium alloy AZ31 in NaCl solution, J. Electrochem. Soc. 163 (2016) C486–C494.
[27] F. Xie, F. Wu, G. Liu, et al., Removal of phosphate from eutrophic lakes through adsorption by in situ formation of magnesium hydroxide from diatomite, Environ. Sci. Technol. 48 (2014) 582–590.
[28] L. Wang, T. Shinohara, B.P. Zhang, Influence of chloride, sulfate and bicarbonate anions on the corrosion behavior of AZ31 magnesium alloy, J. Alloy. Compd. 496 (2010) 500–507.
[29] J. Li, Q. Jiang, H. Sun, et al., Effect of heat treatment on corrosion behavior of AZ63 magnesium alloy in 3.5 wt.% sodium chloride solution, Corros. Sci. 111 (2016) 288–301.
[30] R.Q. Hou, N. Scharnagl, F. Feyerabend, et al., Exploring the effects of organic molecules on the degradation of magnesium under cell culture conditions, Corros. Sci. 132 (2017) 35–45.
[31] M. Kaseem, Y.G. Ko, Morphological modification and corrosion response of MgO and $Mg_3(PO_4)_2$ composite formed on magnesium alloy, Compos. Part B-Eng. 176 (2019) 107225.